J. Plasma Physics (2001), *vol.* 66, *part* 4, *pp.* 259–274. © 2001 Cambridge University Press
DOI: 10.1017/S0022377801001295 Printed in the United Kingdom

A note on the compression ratio in MHD shocks

K. KABIN[1,2]

[1]Department of Atmospheric, Oceanic and Space Sciences, University of Michigan, Ann Arbor, MI, 48109, USA
[2]Present address: Department of Chemistry, University of British Columbia, Vancouver, B.C., Canada V6T 1Z1

(Received 8 August 2000 and in revised form 19 March 2001)

Abstract. We present an analysis of the compression ratio in MHD shocks. Although the equation describing the compression ratio has been in the literature for decades, we believe that our results are interesting and complementary to the earlier research. We concentrate on the behavior of the compression ratio in a bow shock as a function of the angle between the shock normal and the plasma velocity. For this problem, we find non-unique solutions in certain regimes, which we investigate in detail. We also find regimes where the compression ratio in fast bow shocks achieves a local maximum in more than one location. In the last section, we consider the compression ratio in slow shocks and make some conclusions about the shape of the shock in this flow regime.

1. Introduction

In this paper, we present some results concerning the compression ratio in ideal MHD shocks. The Rankine–Hugoniot conditions for MHD have been analyzed by many authors (Anderson 1963; Kennel et al. 1989; DeSterck and Poedts 2000) however we believe that a detailed study of the compression ratio along a bow shock for fixed upstream parameters has not been yet performed.

The shocks in MHD are much more complicated and diverse than in gas dynamics. The basic classification of MHD shocks is illustrated by Fig. 1 (Landau and Lifshitz 1984). The horizontal axis on this diagram is the normal to the shock front component of the speed in front of the shock (u_{n1}) and the vertical axis is the normal component of the speed behind the shock (u_{n2}). The normal components of the slow, Alfvén and fast speeds are marked on the axes as u_s, u_A and u_f. The subscript 1 denotes the speeds in front of the shock (plotted on the horizontal axis) and the subscript 2 refers to the speeds behind the shock (plotted on the vertical axis). All these speeds are calculated in the reference frame moving with the shock.

The axes in Fig. 1 are divided into four intervals by the characteristic speeds u_f, u_A and u_s, commonly denoted by numbers 1 to 4, with 1 being the superfast regime and 4 being subslow. A shock transition is referred to by two numbers describing to which interval the speeds ahead of the shock and behind it belong (also shown in Fig. 1). Points with coordinates (u_{f1}, u_{f2}), (u_{A1}, u_{A2}) and (u_{s1}, u_{s2}) correspond to the fast, Alfvén and slow characteristics respectively. These points are marked in

https://doi.org/10.1017/S0022377801001295 Published online by Cambridge University Press

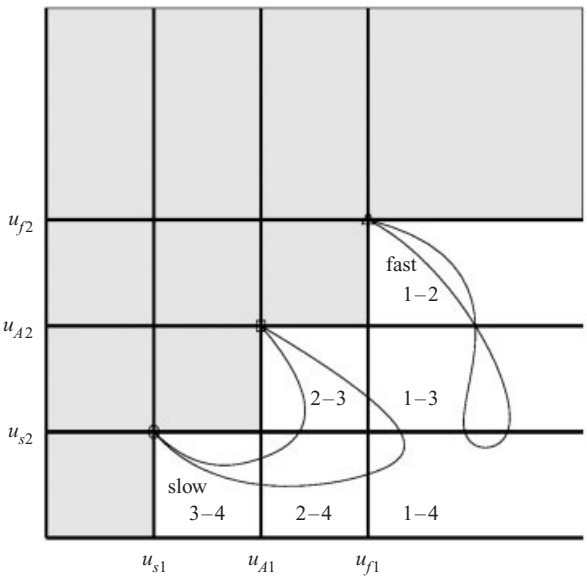


Figure 1. Classification of MHD shocks. The horizontal axis is the speed normal to the shock in front of the shock and the vertical axis is the speed behind the shock. The shaded area corresponds to the shocks prohibited by the entropy condition. Numbers in the white areas describe the type of shock transition. The triangle, square and circle mark the fast, Alfvén and slow characteristics respectively. The thin curved lines represent shocks, shown in Fig. 4 (see text for details).

Fig. 1 by the triangle, square and circle respectively. The thin lines will be discussed later.

The shaded area in Fig. 1 corresponds to the unphysical rarefaction shocks that do not satisfy the entropy condition. In addition to the requirement that the entropy increase across the shock, the so-called evolutionary condition (stability with respect to break-up) is considered to be important in MHD (Akhiezer et al. 1959; Landau and Lifshitz 1984). If a shock is perturbed slightly, this infinitesimal disturbance should be able to propagate away from the shock in the form of linear waves. Whether this is possible or not is checked simply by counting the number of equations (number of the outward-going waves) and the unknowns (variables that can be disturbed). In gas dynamics this analysis does not give anything new; compressive shocks are evolutionary. In MHD, however, only fast (1–2) and slow (3–4) shocks are evolutionary (the number of unknowns equals the number of equations). All other shocks are referred to as intermediate (or non-evolutionary).

The role of the evolutionary condition in MHD is still a matter of active debate. In some numerical calculations, apparently stable intermediate shocks were obtained (Brio and Wu 1988; Wu 1990). However, the evidence from the numerical calculations should be considered with caution because the numerical methods may be introducing some artificial regularization. For example, Barmin et al. (1996) showed that the intermediate wave discussed in Brio and Wu (1988) decays as non-evolutionary under the influence of tangential disturbances, which simply were not allowed in the one-dimensional treatment of the problem by Brio and Wu (1988). At the same time, Kennel et al. (1989) argued that the evolutionary condition does not apply to MHD because this system of equations is not strictly hyperbolic. It was

https://doi.org/10.1017/S0022377801001295 Published online by Cambridge University Press

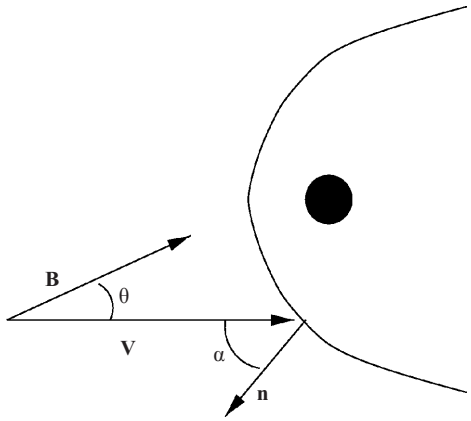


Figure 2. Sketch of the geometry of a typical bow shock.

also shown that non-ideal effects, such as dissipation and resistivity, may stabilize non-evolutionary shocks, at least for small perturbation amplitudes, but the analysis is yet far from being completed (Kennel et al. 1990; Markovskii 1999; DeSterck and Poedts 2000).

2. Compression ratio in an MHD shock

An important parameter describing the strength of a shock is the compression ratio q, defined as the ratio of the density immediately behind the shock to the density in front of the shock.

In this paper we mostly consider the variation of the compression ratio with α: the angle between the shock normal and the plasma velocity. There is clearly a physical motivation for such a consideration: this angle is the only parameter on which the physical quantities behind the bell-shaped bow shock depend (for prescribed uniform upstream conditions) – see Fig. 2. Interestingly, by considering this simple problem, we can make rather non-trivial and far-reaching conclusions concerning the possible shock configurations.

The angle α varies between $\alpha_{\min}$ and $\alpha_{\max}$ which are determined by the linear theory – far from the body, the shock compression ratio becomes unity and the shock itself degenerates into a linear characteristic. For gas dynamics $\alpha_{\max} = -\alpha_{\min} = 90^\circ - \arcsin(1/M_s)$, where M_s is the total upstream sonic Mach number. For MHD in general, $\alpha_{\max} \neq -\alpha_{\min}$. In MHD, there are three non-trivial families of steady-state characteristics (two magnetoacoustic and Alfvén). The magnetoacoustic steady-state characteristics form angles ξ with the direction of the velocity and ψ with the magnetic field, which are defined by the equation (Roe, private communication, 2000):

$$\cos^2\psi = (1 - M_A^2 \sin^2\xi)(1 - M_s^2 \sin^2\xi). \tag{2.1}$$

This equation may be written equivalently as a quartic equation for $\lambda = \tan\xi$ as described for example by Kogan (1960) and Cabannes (1970). Note that in the plane of $\mathbf{B}$ and $\mathbf{u}$, $\psi = \xi - \theta$. Here θ is the angle between the velocity vector and the magnetic field and M_A is the total Alfvénic Mach number, $M_A = u\sqrt{4\pi\rho}/B$. Two roots of this equation are always real; the other two may be complex. If (2.1) has only two real roots, they correspond to the two slow characteristics. If there

https://doi.org/10.1017/S0022377801001295 Published online by Cambridge University Press

are four real roots, they describe either two fast and two slow characteristics, or four slow ones. The asymptotic values of α are related to the solutions of (2.1) as $\alpha_{\min,\max} = -90°\mathrm{sgn}(\xi) + \xi$. The direction of the Alfvén characteristics is defined by the equation

$$\sin\,\theta = (M_A \pm \cos\,\theta)\,\tan\,\xi. \tag{2.2}$$

Alfvén characteristics are always real, regardless of the flow speed.

From Fig. 1 and conservation of mass, it is clear that if there is more than one solution to the Rankine–Hugoniot equations for fixed upstream parameters and shock normal, then the fast shock will be the one with the smallest compression ratio. Unlike gas dynamics, the equation for q in MHD may not be solved easily for oblique shocks. In general, q satisfies the following third-order polynomial equation:

$$\begin{aligned}&(A_1^2 - q)^2\left[A_1^2 - \frac{2qS_1^2}{q+1-\gamma(q-1)}\right]\\ &-qk_1^2A_1^2\left[\frac{2q-\gamma(q-1)}{q+1-\gamma(q-1)}A_1^2 - q\right] = 0.\end{aligned} \tag{2.3}$$

Here $a_s = \sqrt{\gamma P/\rho}$ is the sound speed, $V_A = B_n/\sqrt{4\pi\rho}$ is the Alfvén speed calculated using only the component of the magnetic field normal to the shock, u_n is the plasma speed normal to the shock front,

$$A = \frac{u_n}{V_A} = \frac{M_A\cos(\alpha)}{\cos(\alpha-\theta)}, \quad S = \frac{a_s}{V_A} = \frac{M_A}{M_s\cos(\alpha-\theta)}$$

and

$$k = \frac{B_t}{B_n} = \tan(\alpha-\theta).$$

The subscript 1 on S, A and k indicates that these quantities are based on the parameters upstream of the shock. The subscript t means tangential and n means normal. An equivalent equation for the compression ratio was derived first by Kiselev (1959) and independently by Anderson (1963). Various forms of this equation and its analysis are given in Kalikhman (1967) and Petrinec and Russell (1997). Equation (2.3) may be simplified by a transformation to a special moving frame (De Hoffmann–Teller frame: Landau and Lifshitz 1984); however, this transformation would have to be different at every point of a curved shock. We find it easier work in a fixed reference frame.

Equation (2.3) is a result of manipulating the Rankine–Hugoniot conditions. It describes all kinds of shocks: compression and rarefaction; fast, slow and intermediate. However, the root $q = 1$, which always appears as a solution of the Rankine–Hugoniot conditions, has been excluded from consideration in deriving equation (2.3). Below we consider only compressive shocks ($q > 1$), leaving outside the scope of this paper rotational and tangential discontinuities.

Before starting a general analysis of the compression ratio let us look briefly at parallel shocks. For this case, $k_1 = 0$ ($\theta = \alpha$) and (2.3) splits into two independent equations:

$$q = \frac{(\gamma+1)M_{s1}^2\cos^2\alpha}{2+(\gamma-1)M_{s1}^2\cos^2\alpha}$$

https://doi.org/10.1017/S0022377801001295 Published online by Cambridge University Press

and

$$q = A_1^2 = \frac{u_{1n}^2 4\pi\rho_1}{B_n^2}.$$

The first of these is just the familiar compression ratio in a gas-dynamical shock (because the magnetic field in this case does not appear in the Rankine–Hugoniot conditions), the second corresponds to the so-called 'switch-on' shocks (which have no gas-dynamical analogue). Since we have these simple analytical solutions, the question of evolutionarity of parallel shock may be easily addressed in full. It can be shown (Landau and Lifshitz 1984) that parallel shocks do not satisfy the evolutionary condition if

$$V_{A1} < u_{n1} < \sqrt{\frac{\gamma+1}{\gamma-1}V_{A1}^2 - \frac{2}{\gamma-1}a_{s1}^2}. \tag{2.4}$$

We can obtain an approximation to the switch-on shock solution for small k_1. A straightforward calculation shows that for $k_1 \ll 1$ the cubic equation expands to

$$(q - A_1^2)^2 - \tan^2(\theta-\alpha)\frac{M_{s1}^2 M_{A1}^4 \cos^4\alpha (M_{A1}^2\cos^2\alpha - 1)}{(\gamma+1)M_{s1}^2 - (\gamma-1)M_{s1}^2 M_{A1}^2\cos^2\alpha - 2M_{A1}^2} = 0.$$

Therefore, if the denominator of the fraction is negative, then $q = A_1^2$ is an isolated solution of the cubic (2.3) for $\theta = \alpha$; otherwise, it is a self-intersection point. It is easy to see the relation of this expression to (2.4): the denominator is positive only when the parallel shock is non-evolutionary.

Although $q = A_1^2$ is always a solution of the cubic equation for $k_1 = 0$, the switch-on shocks are not always possible. In a switch-on shock the magnetic field is normal to the shock surface in front of the shock, while behind the shock it has a tangential component (hence the name). It can be shown (Landau and Lifshitz 1984) that B_{t2} behind the shock is given by

$$B_{t2}^2 = \frac{\rho_1}{V_{A1}^2}(u_{n1}^2 - V_{A1}^2)[(\gamma+1)V_{A1}^2 - 2a_s^2 - (\gamma-1)u_{n1}^2].$$

Therefore, one can see that the switch-on shock can exist only when the parallel shock is non-evolutionary. This is illustrated by Fig. 3 for $\gamma = \frac{5}{3}$, $M_s = 5.8$, and $M_A = 2.41666$ (solar wind parameters typical for Mercury; the numerical simulation of Kabin et al. (2000) provided the original motivation for this study).

Now we wish to consider the general case ($\theta \neq \alpha$). In the following study we prescribe the upstream values of M_s, M_A and θ and investigate the dependence of the shock parameters on the angle α. Unlike gas dynamics, the maximum compression ratio in MHD shocks occurs at zero angle of attack α only if the magnetic field is either parallel or perpendicular to the velocity. It can be proved, however, to lie in the plane containing the upstream velocity and magnetic field. Indeed, for an MHD shock, the coplanarity theorem holds (Landau and Lifshitz 1984): the vectors of magnetic field intensity before, $\mathbf{B}_1$, and after, $\mathbf{B}_2$, the shock, the normal to the shock front, $\mathbf{n}$, and the jump in the velocity, $\mathbf{u}_2 - \mathbf{u}_1$, all lie in the same plane. Therefore, the magnitude of the velocity component perpendicular to the plane defined by $\mathbf{B}_1$ and $\mathbf{n}$ does not affect the compression ratio, and the shock has to be symmetric with respect to the $(\mathbf{u}_1, \mathbf{B}_1)$ plane. Thus, the highest compression ratio will be achieved in this plane.

It is known that in certain parameter regimes, the Rankine–Hugoniot relations

https://doi.org/10.1017/S0022377801001295 Published online by Cambridge University Press

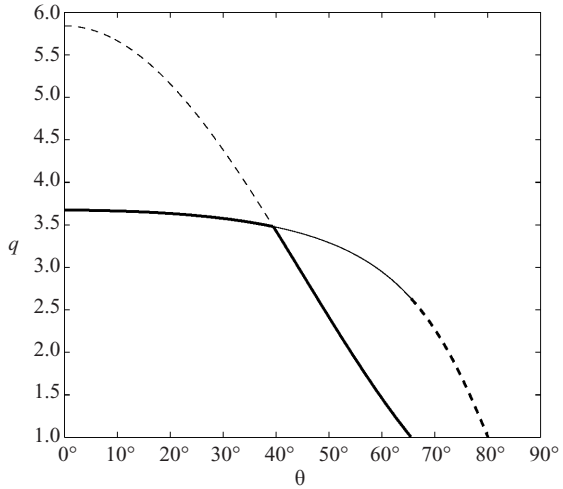


Figure 3. Compression ratio in parallel shocks for $M_s = 5.8$ and $M_A = 2.41666$. The thick line is the fast shock, and the part of the line between 39.48° and 65.557° is the switch-on shock; the thin line is the 1–4 shock, the thick dashed line is the slow shock, and the thin dashed line is the non-existing ($B_{t2}^2 < 0$) switch-on shock.

admit more than one compressive solution (Anderson 1963; Kennel et al. 1989). Figure 4 shows all real solutions of (2.3) as functions of α for the following set of upstream parameters: $M_s = 5.8$, $M_A = 2.41666$, $\gamma = \frac{5}{3}$. The angle between the magnetic field and velocity is $\theta = 42°$. We vary the angle α in the plane defined by the vectors **u** and **B**. The style of the line in Fig. 4 and the numbers next to the curve define the type of the transition. Note that there are zones where the solution is double- and even triple-valued. Figures 4(b) and 5 show in detail the regions where the solution is triple-valued. Of course, for any α, (2.3) has only one solution corresponding to a fast or a slow shock. We note that for different values of parameters, a plot of the compression ratio as a function of α can be a single-valued curve (as it always is in gas dynamics) – examples for the same Mach and Alfvén numbers and $\theta = 0°$, $\theta = 20°$ are given in Kabin et al. 2000.

McKenzie and Westphal (1969) studied the transmission coefficients for the Alfvén wave impinging on a fast shock. Their formulas for the ratio of the amplitudes of the forward-propagating Alfvén wave behind the shock (in this problem, behind the shock there are always forward- and backward-propagating waves) to that in front of the shock may be written in the form:

$$\frac{\delta B_2}{\delta B_1} = \frac{(M_{A1} + 1)(\sqrt{q} - 1)}{2(M_{A1}/\sqrt{q} - 1)}.$$

One can see that this expression becomes singular for the switch-on shock (self-intersection point on Fig. 4). This indicates the probable instability of bow shocks in regimes where the parallel shock wave is non-evolutionary. It is quite possible, then, that the local structure of the flow and MHD discontinuities will change significantly. Numerical calculations of the plasma flows involving complicated multiple shocks in these regimes can be found in DeSterck et al. (1999) and DeSterck and Poedts (2000).

There are six points in Fig. 4 for which the compression ratio becomes 1. They are

https://doi.org/10.1017/S0022377801001295 Published online by Cambridge University Press

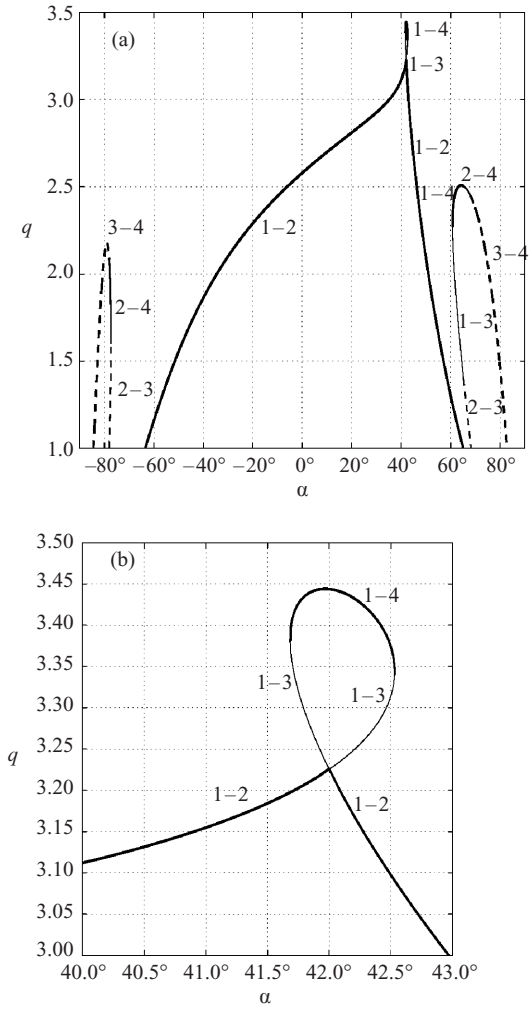


Figure 4. (a) Compression ratio for $M_s = 5.8$, $M_A = 2.41666$, $\gamma = \frac{5}{3}$ and $\theta = 42°$. Numbers and line type indicate the type of the shock transition. (b) A detail of (a).

the directions of the linear characteristics, which can be found by solving (2.1) and (2.2). For the above values of Mach and Alfvénic Mach numbers, the fast and slow characteristic directions are $-63.4976°$, $65.1517°$, $-84.4436°$ and $82.7894°$. The first two of the four correspond to the fast characteristics; at these values of α, the fast shock in Fig. 4 starts and ends. The last two describe the slow characteristics; at the corresponding values of α, the compression ratio in the slow shocks becomes 1. The directions of the Alfvén characteristics are $-78.0435°$ and $68.2068°$. These are the values at which 2–3 shocks in Fig. 4 end. It is clear from Fig. 1 that only 1–2 (fast), 3–4 (slow) and 2–3 transitions may have the compression ratio 1.

It is useful to analyze different shock transitions shown in Fig. 4 in the (u_{1n}, u_{2n}) plane as shown in Fig. 1. The thin continuous lines in Fig. 1 represent the three shock branches shown in Fig. 4. Each of these lines goes from one characteristic point to another (or back to the same point). There are two lines starting at each characteristic point because each family consists of two characteristics. Note that

https://doi.org/10.1017/S0022377801001295 Published online by Cambridge University Press

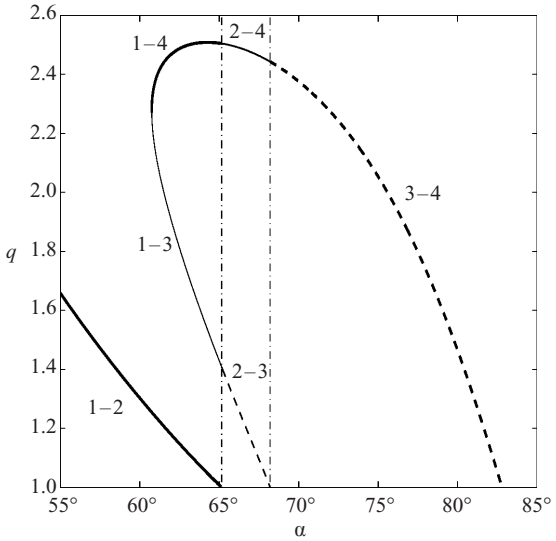


Figure 5. Compression ratio for $M_s = 5.8$, $M_A = 2.41666$, $\gamma = 5/3$ and $\theta = 42°$. The left and right dash-dotted vertical lines correspond to the fast and Alfvén characteristics respectively. The numbers and line types indicate the type of the shock transition.

this figure is just a cartoon, since for different angles α, the ratios between the fast, slow and Alfvén speeds change. Therefore, the scales of the axis in Fig. 1 should change as well. However, we believe that the schematics in Fig. 1 are useful for understanding, for example, the sequence of the shock transition for different parameters.

We can understand at which values of α the transition between different types of shocks occurs by examining Fig. 5. It shows an enlarged view of part of Fig. 4(a). The right branch from Fig. 4(a) was chosen since it is more complicated than the left one and demonstrates a larger number of transitions. The two vertical dash–dotted lines correspond to the fast and Alfvén characteristics, which clearly coincide with the changes in the type of the shocks. An additional transition (from 1–4 type to 1–3 type) occurs at the point where the slope of the compression ratio becomes infinite. This is clearly the order in which one of the curves in Fig. 1 cuts through different domains. It starts at the point corresponding to the slow characteristic, and ends at the Alfvén characteristic. A continuous curve with these endpoints should go at least through 3–4, 2–4 and 2–3 domains; this is the route followed by the left branch from Fig. 4(a). Alternatively, it can make a larger loop and go through 3–4, 2–4, 1–4, 1–3 and 2–3 domains, like the right branch from Fig. 4(a) does. Finally, the central branch from Fig. 4(a) starts as a 1–2 shock, then goes into 1–3 and 1–4 domains, returns into 1–3 domain again, and suffers a self-intersection on the border before becoming a fast shock again. One can expect that there are other ways to connect fast, slow and Alfvén characteristics in Fig. 1. As we will show later (Fig. 6), some of these different possibilities do occur.

As the angle θ between the velocity and the magnetic field increases, the picture shown in Fig. 4 stays qualitatively the same for a while: it has one self-intersecting curve and two disconnected branches on the left and right. However, when θ reaches a certain critical value, equal to 46° for $M_s = 5.8$ and $M_A = 2.4166666$, the structure undergoes another morphological change.

https://doi.org/10.1017/S0022377801001295 Published online by Cambridge University Press

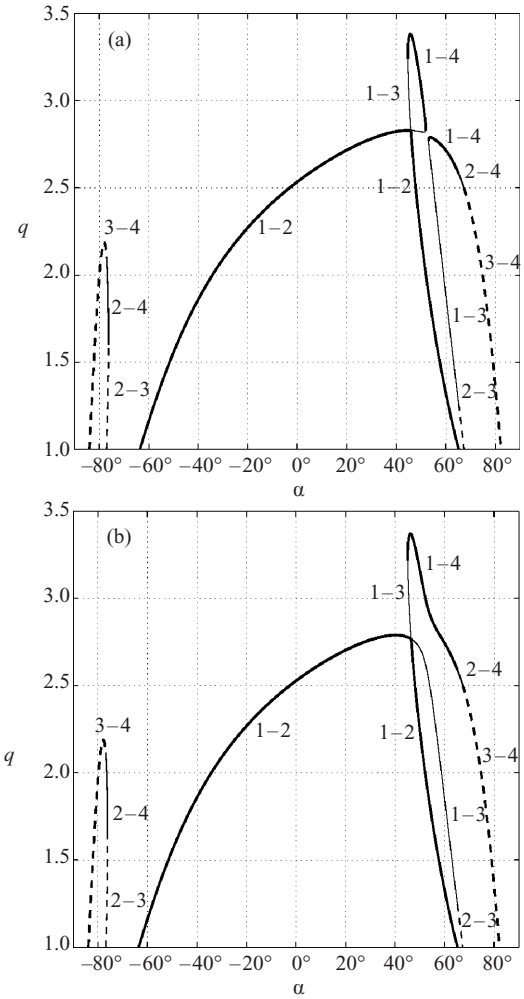


Figure 6. Same as Fig. 4: (a) $\theta = 45.9°$; (b) $\theta = 46.1°$.

Figure 6(a) shows the compression ratio for $\theta = 45.9°$ and Fig. 6(b) the compression ratio for $\theta = 46.1°$. For $\theta = 45.9°$, there is still a curve with a self-intersection, although the loop is very distorted and is almost touching the intermediate–slow branch. For $\theta = 46.1°$, the two curves have 'reconnected'. Now there are two distinct crossing curves, neither of which has self-intersections. As θ increases further, the two curves start to move away from each other, and at $\theta = 65.5°$ they stop crossing each other. Up to this point, the fast-shock compression ratio has a point of discontinuous slope at the switch-on shock; for $\theta > 65.5°$, the compression in a fast shock wave is a smooth curve once again. At the same angle θ, the parallel shock becomes evolutionary once again, but it is a slow shock now.

Figure 7 shows the maximum compression ratio in a fast shock as a function of the angle between velocity and magnetic field θ for $M_s = 5.8$ and $M_A = 2.41666$. There are two points in Fig. 7 where the slope of the curve changes discontinuously: $\theta = 39.5°$ and $\theta = 46°$. At the first of these, the intermediate shock loop appears for the first time near a parallel shock; for the second, the next morphological change (shown in Fig. 6) occurs.

https://doi.org/10.1017/S0022377801001295 Published online by Cambridge University Press

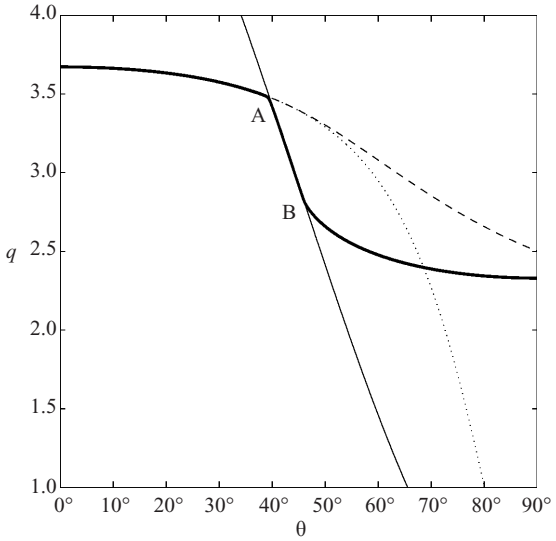


Figure 7. Maximum compression ratio in MHD shocks for $M_s = 5.8$ and $M_A = 2.41666$ as a function of the angle θ between velocity and magnetic field. The thick solid line corresponds to fast shocks. The part of the line between the points A and B is a switch-on shock (shown by a thin line). Above the point A, the switch-on shock cannot exist because the formal solution gives $B_{t2}^2 < 0$. It exists below the point B as a fast shock, but the maximum compression ratio is achieved elsewhere on the fast shock. The dashed line corresponds to the 1–4 shocks. The dotted line is the non-evolutionary part of the parallel shock.

Figure 8 shows the angle α_M between the shock normal and the velocity where the maximum compression ratio is achieved for $M_s = 5.8$ and $M_A = 2.41666$ (thick continuous and dashed lines). The thin line on the same plot corresponds to $M_s = 5.0$ and $M_A = 4.16666$; for these parameters, no intermediate shocks appear and the angle corresponding to the maximum compression ratio in a fast shock is just a single smooth curve with a single maximum. As one expects, $\alpha_M = 0$ when $\theta = 0$ or $\theta = 90°$. In all the cases we have investigated, the maximum compression ratio occurs between the points where the velocity is normal to the shock and where the magnetic field is normal to the shock. For small θ, the maximum compression ratio often occurs very close to a parallel shock; the thick line in Fig. 8 is an example.

Another example of curious behavior of the compression ratio in an MHD shock can be seen in Fig. 9. It corresponds to $M_s = 10$, $M_A = 4.16666$, $\gamma = \frac{5}{3}$ and $\theta = 63°$. For these parameters, no intermediate shocks occur in the region of existence of the fast shock – the fast shock is just a simple single curve without any self-intersections, only a fragment of which is shown in Fig. 9. However, one can see that the compression ratio reaches two local maxima, separated by a minimum. The maximum near the parallel shock is much narrower and steeper than the other one, but, as Fig. 9(b) shows, it is still a smooth curve rather than a cusp.

3. Numerical example

To illustrate our theoretical findings, we have performed a numerical simulation of the plasma flow past a superconducting sphere using a finite-volume Godunov-type ideal MHD code. The particularities of the numerical method are described in

https://doi.org/10.1017/S0022377801001295 Published online by Cambridge University Press

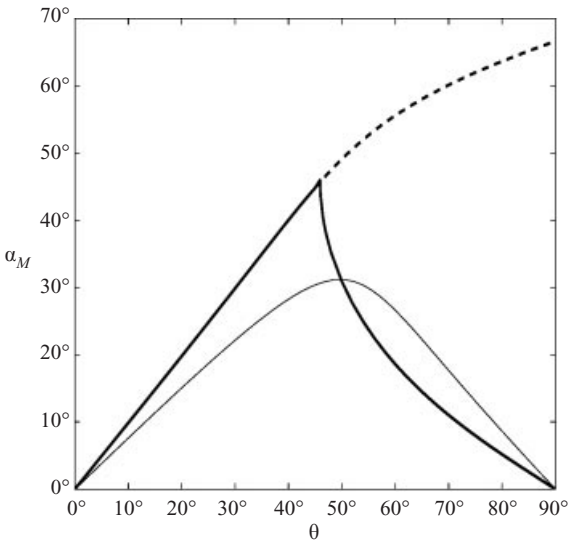


Figure 8. Angle α_M between the shock normal and the velocity where the maximum compression ratio in a fast shock is achieved as a function of the angle θ between velocity and magnetic field. The thick solid line corresponds to a fast shock with $M_s = 5.8$ and $M_A = 2.41666$, the dashed line to intermediate and slow shocks with the same Mach and Alfvén numbers and the thin line to $M_s = 5.0$ and $M_A = 4.16666$.

Powell et al. (1999). The numerical viscosity and resistivity of the method appear to be sufficient to stabilize the intermediate shocks in our simulations.

The upstream parameters are $M_s = 5.8$, $M_A = 2.2$ and $\theta = 25°$. For these parameters, the compression ratio as a function of α has the same general form as that in Fig. 6(b). The results (density contours) of the numerical calculation in the plane defined by the velocity and magnetic field vectors are shown in Fig. 10(b). For easier understanding, Fig. 10(a) is a schematic explaining the flow structure. The arc AB is the fast shock; at point B, the magnetic field is normal to the shock front – here a switch-on shock occurs. The arc BC consists of the intermediate 1–3 and 2–3 shocks. The area CBD in front of the intermediate shocks is filled by a rarefaction wave. The line BD is the fast characteristic line of the flow. Because the part BC of the shock front is formed by the intermediate shocks, there can be a disturbance associated with the fast mode upstream of this shock. One can clearly see from Fig. 10(b) that the arc BC is an intermediate shock from the way in which the magnetic field is refracted.

This structure of the flow past a sphere is similar to that discussed by DeSterck and Poedts (1999b, 2000); however, they considered smaller Mach numbers and angles between the magnetic field and velocity. Their solutions have a fast shock or a fast shock followed by a rarefaction wave, where we find only a rarefaction wave.

4. Slow shocks

Finally, we briefly discuss slow shocks in one specific regime. It turns out that just by solving (2.3), we can make some rather non-trivial conclusions about these.

Slow shocks in MHD are very interesting. They do not have an analogy in gas dynamics, which makes them somewhat counterintuitive. Slow shocks are possible

https://doi.org/10.1017/S0022377801001295 Published online by Cambridge University Press

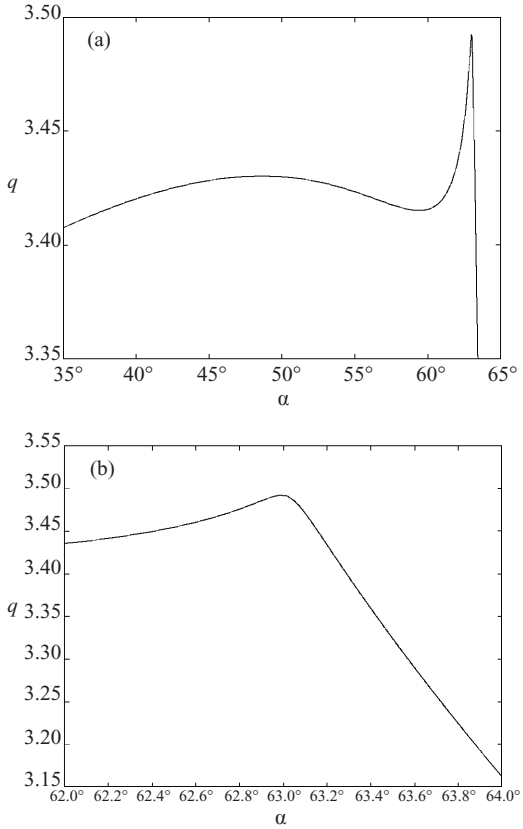


Figure 9. (a) Compression ratio in a fast shock for $M_s = 10$, $M_A = 4.16666$, $\gamma = \frac{5}{3}$ and $\theta = 63°$. (b) A detail of (a), showing that the right maximum is a smooth curve, rather than a cusp.

for any combination of plasma flow parameters, except for the super-Alfvénic flows with the velocity parallel to the magnetic field. They are often directed upstream, which never happens in gas dynamics.

There is no evidence that slow shocks ever constitute a large-scale bow shock in front of a body. Nevertheless, they are a vital part of the flow near magnetic reconnection in most models (Petschek 1964). They also seem to appear in complicated shock interactions, such as described by DeSterck (1999). Finally, there are observations that can be interpreted as detection of slow shocks in the Earth's magnetosphere (e.g. Song et al. 1992; Saito et al. 1995).

For flows with magnetic field parallel to the plasma velocity, there are two distinct domains of hyperbolicity for steady flows (Cabannes 1970). One is for plasma speed larger than $\max(a_s, V_A)$, and we can expect fast shocks to be most important in this regime. The other occurs for $a_s V_A/\sqrt{a_s^2 + V_A^2} < u < \min(a_s, V_A)$, when fast shocks are impossible and the flow has to be dominated by the slow shocks. Below we consider an example of this type of flow with the following upstream parameters: $M_s = 0.9$, $M_A = 0.75$, $\mathbf{B} \parallel \mathbf{u}$, $\gamma = \frac{5}{3}$. As before, solving (2.3), we study how the parameters of the plasma behind a slow shock are related to the parameters in front of it.

https://doi.org/10.1017/S0022377801001295 Published online by Cambridge University Press

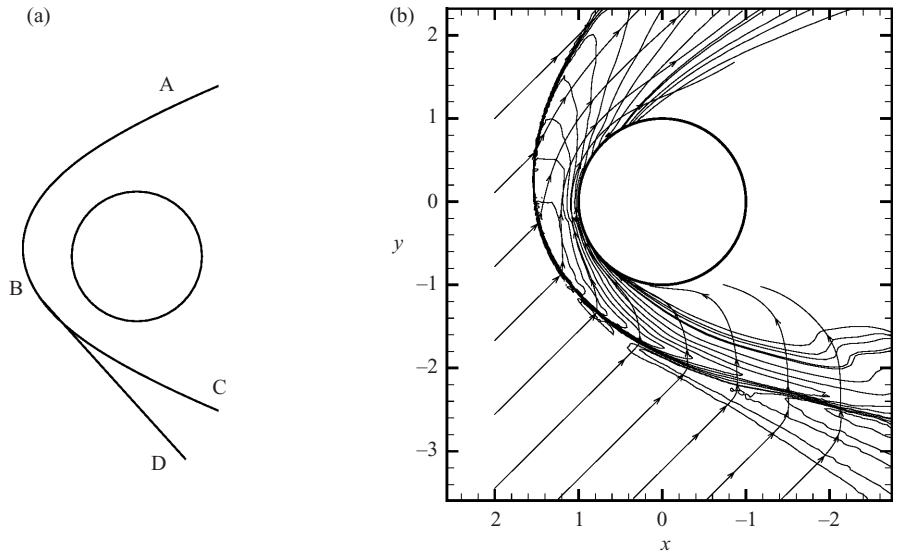


Figure 10. (a) Schematic of the flow past a superconducting sphere. AB is a fast shock, B is a switch-on shock, BC is an intermediate shock and BD is a fast characteristic. The area CBD is filled by a rarefaction wave. (b) Density contours and magnetic field lines from a numerical simulation with $M_s = 5.8$, $M_A = 2.2$ and $\theta = 45°$.

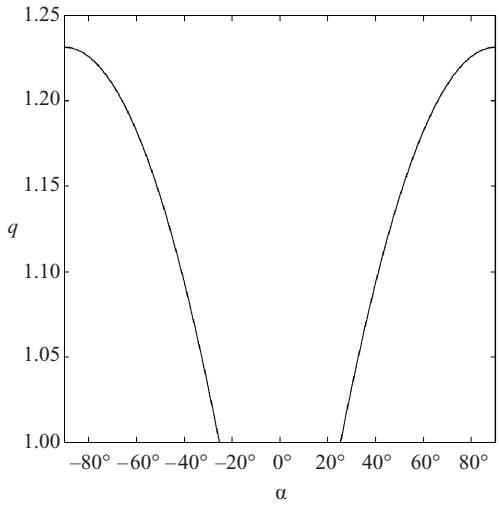


Figure 11. Compression ratio as a function of angle α in a slow shock for $M_s = 0.9$, $M_A = 0.75$ and $B \parallel v$.

Figure 11 is similar to Fig. 4 for the slow shock. One can see immediately a striking difference. There are no solutions with plasma velocity perpendicular to the shock surface. Contrary to either fast shocks or gas-dynamic shocks, the compression ratio increases with α and reaches its maximum for the case when the plasma velocity is parallel to the shock front. The only way we can imagine this happening in a flow past a body is if the sub-ram point of the shock is actually a cusp, as shown in Fig. 12(a). This figure also shows the refraction of the streamlines in the

https://doi.org/10.1017/S0022377801001295 Published online by Cambridge University Press

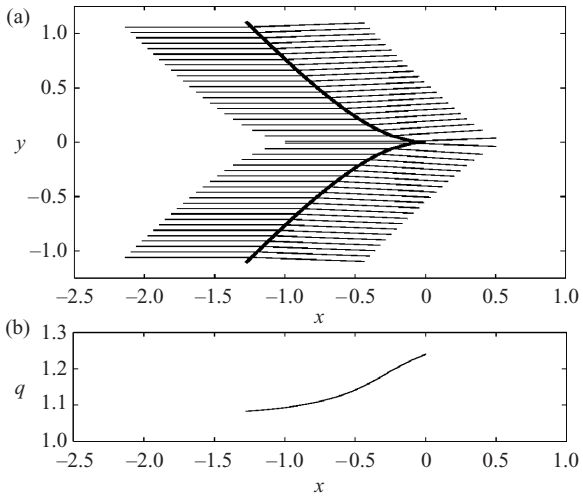


Figure 12. (a) A sketch of the geometry of an upstream-going slow shock (bold line) and the streamlines (thin lines). (b) Compression ratio in this shock. The parameters are the same as for Fig. 11.

shock. The length of the streamlines before they enter the shock corresponds to the uniform upstream flow and after the shock to the velocity magnitude calculated from the Rankine–Hugoniot relations. Figure 12(b) shows the compression ratio in this shock.

Of course, just by solving (2.3) we cannot get any information about the shape of the shock; for that we need to solve the MHD equations for certain boundary conditions. The shock shape in Fig. 12 is just a cartoon (it is composed of two sections of a hyperbola, adjusted to have a cusp point in proper place and the correct asymptotic slope for large negative x). The results of the solution of (2.3) are plotted at the points where the shock has appropriate slope.

It is interesting to point out that very similar concave-outward shocks were observed in numerical simulations of DeSterck and Poedts (1999a) of field-aligned MHD flows over both cylinder and sphere.

5. Conclusions

We have investigated the compression ratio in MHD shocks, which is described by a third-order equation. We found regimes, when none of the three possible solutions may be excluded from the consideration by simple arguments, such as increase of entropy across the shock or physical admissibility of the downstream parameters. These multiple solutions correspond to intermediate (non-evolutionary) shocks. One of the possibilities is that, in these regimes, the bow shock in front of a body would have a significantly different morphology than a typical bell-shaped shock. It may include multiple shocks as described by DeSterck and Poedts (1999b, 2000) or a rarefaction wave as shown in Fig. 10. We have also found a regime when the compression ratio in a bow shock has two local maxima. One of these maxima is higher, but much more narrow. Resolving such a maximum numerically may require significant computational resources.

We would like to point out that the appearance of multiple maxima in a compres-

https://doi.org/10.1017/S0022377801001295 Published online by Cambridge University Press

sion ratio, or unusual structures in a numerical simulation, may be confused with a carbuncle-like phenomenon, or some other manifestation of nonlinear numerical instabilities.

Finally, we have investigated the behavior of the compression ratio in a slow shock. Interestingly, this simple analysis allowed us to make some rather non-trivial conclusions about the possible shapes of slow shocks. We are led to expect that such shocks would have cusp points.

Acknowledgements

I would like to acknowledge many stimulating discussions with P. L. Roe, T. I. Gombosi, and G. Atkinson, and the helpful suggestions of the anonymous referee.

References

Akhiezer, A. I., Lubarskii, G. J. and Polovin, R. V. 1959 The stability of shock waves in magnetohydrodynamics. *Soviet Phys. JETP* **8**, 507–511.

Anderson J. E. 1963 *Magnetohydrodynamic Shock Waves*. Cambridge, MA: MIT Press.

Barmin, A. A., Kulikovskiy, A. G. and Pogorelov, N. V. 1996 Shock-capturing approach and nonevolutionary solutions in magnetohydrodynamics. *J. Comput. Phys.* **126**, 77–90.

Brio, M. and Wu, C. C. 1988 An upwind differencing scheme for the equations of ideal magnetohydrodynamics. *J. Comput. Phys.* **75**, 400–422.

Cabannes, H. 1970 *Theoretical Magnetofluiddynamics*. New York: Academic Press.

DeSterck, H. 1999 Numerical simulation and analysis of magnetically dominated MHD bow shock flows with applications in space physics. PhD thesis, Katholieke Universiteit Leuven.

DeSterck, H. and Poedts, S. 1999a Field-aligned magnetohydrodynamic bow shock flows in the switch-on regime. *Astron. Astophys.* **343**, 641–649.

DeSterck, H. and Poedts, S. 1999b Stationary slow shocks in the magnetosheath for solar wind conditions with $\beta < 2/\gamma$: Three-dimensional MHD simulations. *J. Geophys. Res.* **104**, 22,401–22,406.

DeSterck, H. and Poedts, S. 2000 Intermediate shocks in three-dimensional magnetohydrodynamic bow-shock flows with multiple interacting shock fronts. *Phys. Rev. Lettr.* **84**, 5524–5527.

DeSterck, H., Deconinck, H., Poedts, S. and Roose, D. 1999 A bow shock flow containing (almost) all types of (exotic) MHD Discontinuities. *Int. Ser. Numer. Maths* **129**, 195–204.

Kabin, K., Gombosi, T. I., DeZeeuw, D. L. and Powell, K. G. 2000 Interaction of Mercury with the solar wind. *Icarus* **143**, 397–406.

Kalikhman, L. E. 1967 *Elements of Magnetogasdynamics*. Philadelphia: Saunders.

Kennel, C. F., Blandford, R. D. and Coppi, P. 1989 MHD intermediate shock discontinuities. Part 1. Rankine–Hugoniot conditions. *J. Plasma Phys.* **42**, 299–319.

Kennel, C. F., Blandford, R. D. and Wu, C. C. 1990 Structure and evolution of small-amplitude intermediate shock waves. *Phys. Fluids* **B2**, 253–269.

Kiselev, M. I. 1959 On the calculation of shock waves in magnetofluid dynamics. *Dokl. Akad. SSSR* **126**, 524–527.

Kogan, M. N. 1960 On the vortices and currents in magnetofluid dynamics. *Dokl. Akad. Nauk SSSR* **139**, 58–59.

Landau, L. D. and Lifshitz, E. M. 1984 *Electrodynamics of Continuous Media*. Oxford: Pergamon.

McKenzie, J. F. and Westphal, K. O. 1969 Transmission of Alfvén waves through the Earth's bow shock. *Planet. Space Sci.* **17**, 1029–1037.

Markovskii, S. A. 1999 Nonevolutionarity of trans-Alfvénic shocks in a magnetized plasma. *J. Geophys. Res.* **104**, 4427–4436.

Petrinec, S. M. and Russell, C. T. 1997 Hydrodynamic and MHD equations across the bow shock and along the surfaces of planetary obstacles. *Space Sci. Rev.* **79**, 757–791.

https://doi.org/10.1017/S0022377801001295 Published online by Cambridge University Press

Petschek, H. E. 1964 Magnetic field annihilation. In: *The Physics of Solar Flares* (ed. W. H. Ness). NASA SP-50.

Powell, K. G., Roe, P. L., Linde, T. J., Gombosi, T. I. and DeZeeuw, D. L. 1999 A solution-adaptive upwind scheme for ideal magnetohydrodynamics. *J. Comput. Phys.* **154**, 284–309.

Saito, Y., Mukai, T., Terasawa, T., Nishida, A., Machida, S., Hirahara, M., Maezawa, K., Kokubun, S. and Yamamoto, T. 1995 Slow-mode shocks in the magnetotail. *J. Geophys. Res.* **100**, 23 567–23 581.

Song, P., Russell, C. T. and Thomsen, M. F. 1992 Slow mode transition in the frontside magnetosphere. *J. Geophys. Res.* **97**, 8295–8305.

Wu, C. C. 1990 Formation, structure, and stability of MHD intermediate shocks. *J. Geophys. Res.* **95**, 8149–8175.

https://doi.org/10.1017/S0022377801001295 Published online by Cambridge University Press